PNAS RESEARCH ARTICLE | IMMUNOLOGY AND INFLAMMATION

Transcription factor C/EBPα is required for the development of Ly6C^{hi} monocytes but not Ly6C^{lo} monocytes

Sunkyung Kim[a], Jing Chen[a], Feiya Ou[a], Tian-Tian Liu[a], Suin Jo[a], William E. Gillanders[a], Theresa L. Murphy[a], and Kenneth M. Murphy[a,1]

Contributed by Kenneth M. Murphy; received September 11, 2023; accepted February 26, 2024; reviewed by Shizuo Akira and Ellen V. Rothenberg

Monocytes comprise two major subsets, Ly6C^{hi} classical monocytes and Ly6C^{lo} nonclassical monocytes. Notch2 signaling in Ly6C^{hi} monocytes triggers transition to Ly6C^{lo} monocytes, which require *Nr4a1*, *Bcl6*, *Irf2*, and *Cebpb*. By comparison, less is known about transcriptional requirements for Ly6C^{hi} monocytes. We find transcription factor CCAAT/enhancer-binding protein alpha (C/EBPα) is highly expressed in Ly6C^{hi} monocytes, but down-regulated in Ly6C^{lo} monocytes. A few previous studies described the requirement of C/EBPα in the development of neutrophils and eosinophils. However, the role of C/EBPα for in vivo monocyte development has not been understood. We deleted the *Cebpa* +37 kb enhancer in mice, eliminating hematopoietic expression of C/EBPα, reproducing the expected neutrophil defect. Surprisingly, we also found a severe and selective loss of Ly6C^{hi} monocytes, while preserving Ly6C^{lo} monocytes. We find that BM progenitors from *Cebpa* +37$^{-/-}$ mice rapidly progress through the monocyte progenitor stage to develop directly into Ly6C^{lo} monocytes even in the absence of Notch2 signaling. These results identify a previously unrecognized role for C/EBPα in maintaining Ly6C^{hi} monocyte identity.

C/EBPα | classical monocyte | nonclassical monocyte | neutrophil | transcription factor

Significance

Ly6C^{lo} monocytes, also known as "patrolling monocytes," develop from Ly6C^{hi} monocytes and play an important protective role in the surveillance of the vascular endothelium. The development of Ly6C^{lo} monocytes is still incompletely understood. We now demonstrate that the transcription factor CCAAT/enhancer-binding protein alpha (C/EBPα) acts to maintain Ly6C^{hi} monocytes and to repress Ly6C^{lo} monocyte development, adding to our understanding of this protective monocyte subset.

Murine monocyte subsets include Ly6C^{hi} CCR2^{+} 'classical' monocytes and Ly6C^{lo} CCR2^{-} "nonclassical" (or patrolling) monocytes (1–3), which differ in both their surface markers and transcriptional profiles (4). Ly6C^{hi} monocytes develop from a common monocyte progenitor (cMoP) (5, 6) in the bone marrow (BM) and have a half-life in circulation of around 1 d (7, 8). Ly6C^{hi} monocytes contribute to tissue-resident macrophages (8–10) and can generate monocyte-derived dendritic cells (MoDCs) (11–14). In turn, Ly6C^{lo} monocytes arise from Ly6C^{hi} monocytes (4, 8, 15) and can be induced by Notch2 signaling upon encounter with ligands in the circulation (16–18). Ly6C^{lo} monocytes require CX3CR1 for survival (19) and provide surveillance and protection for vascular endothelium (3, 20–23).

The transcriptional requirements for monocyte development are incompletely understood. The cMoP (5, 6) arise convergently from GMPs (6, 10) and monocyte-dendritic cell progenitors (MDPs) (15, 24) but the basis for cMoP specification has not been described. Known requirements for Ly6C^{hi} monocyte development include PU.1 (25), IRF8 (26), and KLF4 (27, 28). PU.1 deficiency causes broad defects in myeloid and lymphoid lineages, while IRF8 deficiency reduces monocyte numbers (26) and causes the accumulation of an immature Kit^{+} cMoP population (29, 30). PU.1 and IRF8 cooperate to support the expression of KLF4, which acts downstream in development and is required for the maturation of monocyte progenitors (26). However, the specific actions of KLF4 in Ly6C^{hi} monocyte development are still unknown.

The known requirements for Ly6C^{lo} monocyte development include transcription factors NUR77 (31), C/EBPβ (4), NOTCH2 (16–18), BCL6, and IRF2 (18). NUR77, C/EBPβ, and BCL6 are expressed more highly in Ly6C^{lo} monocytes than in Ly6C^{hi} monocytes (4, 18). C/EBPβ is required for survival for Ly6C^{lo} monocytes, but not Ly6C^{hi} monocytes (4, 32, 33) and may support the expression of the *Nr4a1* gene encoding NUR77 (4) or of macrophage colony-stimulating factor receptor (M-CSFR) (CD115/*Csf1r*) (33). Germline *Nr4a1* deficiency (31) and early myeloid-specific deletion of *Bcl6* (18) eliminate the development of Ly6C^{lo} monocytes but not of Ly6C^{hi} monocytes. Notch2 signaling induces the transition of Ly6C^{hi} monocytes into Ly6C^{lo} monocytes (16–18). However, the relevant targets of Notch signaling and the interplay between NUR77, BCL6, and C/EBPβ in the transition from Ly6C^{hi} to Ly6C^{lo} monocytes remain unclear.

C/EBPα is a potent transcription factor to direct specification of myeloid lineages (34). C/EBPα deficiency causes the loss of granulocyte-macrophage progenitors (GMPs) (35–37), which could affect both granulopoiesis and monopoiesis. The previous studies showed defects in the development of mature neutrophils and eosinophils upon C/EBPα deficiency

Author affiliations: [a]Department of Pathology and Immunology, Washington University in St. Louis School of Medicine, St. Louis, MO

Author contributions: S.K., T.L.M., and K.M.M. designed research; S.K., J.C., F.O., T.-T.L., S.J., W.E.G., and T.L.M. performed research; S.K., F.O., T.-T.L., and T.L.M. contributed new reagents/analytic tools; S.K., J.C., F.O., T.-T.L., S.J., W.E.G., T.L.M., and K.M.M. analyzed data; and S.K., T.L.M., and K.M.M. wrote the paper.

Reviewers: S.A., Osaka Daigaku; and E.V.R., California Institute of Technology.

The authors declare no competing interest.

[1]To whom correspondence may be addressed. Email: kmurphy@wustl.edu.

This article contains supporting information online at https://www.pnas.org/lookup/suppl/doi:10.1073/pnas.2315659121/-/DCSupplemental.

Published April 2, 2024.

without notable impacts on monocyte development. However, these studies did not examine Ly6C^{hi} and Ly6C^{lo} monocyte subsets separately. Since we observed that C/EBPα expression is down-regulated during the transition of Ly6C^{hi} monocytes into Ly6C^{lo} monocytes, we asked whether C/EBPα played any role in monocyte development. We generated mice with a deletion in the *Cebpa* +37 kb enhancer that abrogates hematopoietic expression of C/EBPα, similar to previous studies (36, 37). As expected, we observe severe defects in granulocyte progenitors and neutrophil development. Additionally, we now report a previously unrecognized and selective requirement for C/EBPα in cMoP and Ly6C^{hi} monocyte development, while Ly6C^{lo} monocytes remain intact. We find that *Cebpa* +37$^{-/-}$ BM progenitors rapidly pass through the cMoP and Ly6C^{hi} monocyte stages and spontaneously progress to Ly6C^{lo} monocytes independently of Notch signaling. These results indicate that C/EBPα maintains Ly6C^{hi} monocyte identity and acts to halt spontaneous Notch-independent progression into Ly6C^{lo} monocytes.

Results

Ly6C^{hi} Monocytes Extinguish C/EBPα Expression on the Transition to Ly6C^{lo} Monocytes. We first examined the pattern of expression for C/EBPα and C/EBPβ at various stages of monocyte development (Fig. 1 and *SI Appendix,* Fig. S1 *A–D*). Intracellular staining (ICS) of BM progenitors showed minimal C/EBPα expression in Lin^{-} Sca-1^{+} cKit^{hi} population (LSK) (38) that were either CD135^{-} or CD135^{+} and showed increasing expression in GMP and MDP (Fig. 1*A*). C/EBPα expression was maximal in the cMoP and showed slightly reduced expression in BM and splenic Ly6C^{hi} monocytes. Notably, C/EBPα expression was abruptly extinguished in BM and splenic Ly6C^{lo} monocytes (Fig. 1*A*). A similar pattern was evident for Ly6C^{hi} and Ly6C^{lo} monocytes in the blood (Fig. 1*B*). C/EBPβ expression showed a distinct pattern from C/EBPα. C/EBPβ was expressed at very low levels in all BM progenitors including the BM Ly6C^{hi} monocytes (Fig. 1*A*). However, splenic and blood Ly6C^{hi} monocytes induced C/EBPβ expression to an intermediate level, which was further increased in the splenic and blood Ly6C^{lo} monocytes (Fig. 1 *A–C*).

We next asked whether these patterns of expression were maintained during the in vitro culture and development of BM monocyte progenitors (Fig. 2). First, we examined the induction of Ly6C^{lo} monocytes from cKit^{hi} BM progenitors developing in vitro on OP9 stromal cells (*SI Appendix,* Fig. S1*E*), as recently described (18). Culture of progenitors on OP9 expressing the Notch ligand Delta-like 1 (DLL1) selectively induced progenitors to lose Ly6C and to acquire CD11c expression (*SI Appendix,* Fig. S1*E*). Using this condition, we examined the expression of C/EBPα and C/EBPβ in monocyte populations developing in these cultures (Fig. 2 *A* and *B*). In agreement with our in vivo observations, Ly6C^{lo} monocytes extinguish expression of C/EBPα during the transition from Ly6C^{hi} monocytes. In addition, purified Ly6C^{hi} monocytes also extinguish C/EBPα expression during induction of MoDC development (Fig. 2 *C* and *D* and *SI Appendix,* Fig. S1 *F* and *G*).

A 552 bp Deletion in the *Cebpa* +37 kb Enhancer Abolishes C/EBPα Expression in BM. To examine the role of C/EBPα in monocyte development, we recreated an enhancer mutation previously described that abrogates C/EBPα expression in hematopoietic lineages (36, 37) (*SI Appendix,* Fig. S2). One of these previous

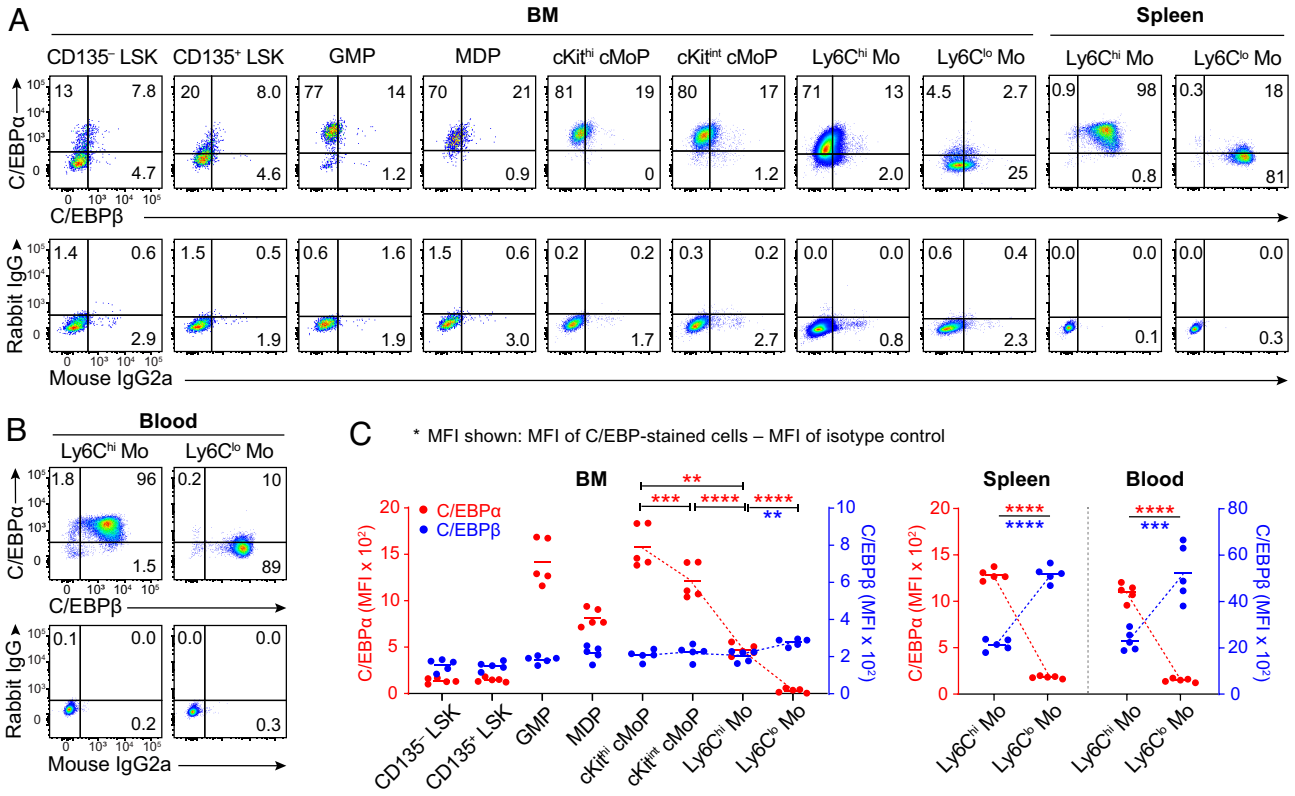

Fig. 1. Ly6C^{hi} monocytes down-regulate C/EBPα expression upon transition to Ly6C^{lo} monocytes. (*A* and *B*) Expression of C/EBPα and C/EBPβ iby the BM progenitors and monocytes in the (*A*) BM and spleen, and (*B*) peripheral blood was analyzed by intracellular staining (*Upper*). Negative gating in the quadrant plots was based on the isotype control of each cell population (*Lower*). Numbers in the plots are percentages of cells in each quadrant. (*C*) Scatter plots show geometric mean fluorescence intensity (MFI) of C/EBPα (red dots and lines) and C/EBPβ (blue dots and lines) of the indicated cell populations in the BM, spleen, and blood (average MFI). The Individual mice are shown as dots. Data shown are a representative of two similar experiments. $^{**}P < 0.01$, $^{***}P < 0.001$, $^{****}P < 0.0001$ (Student's *t* test).

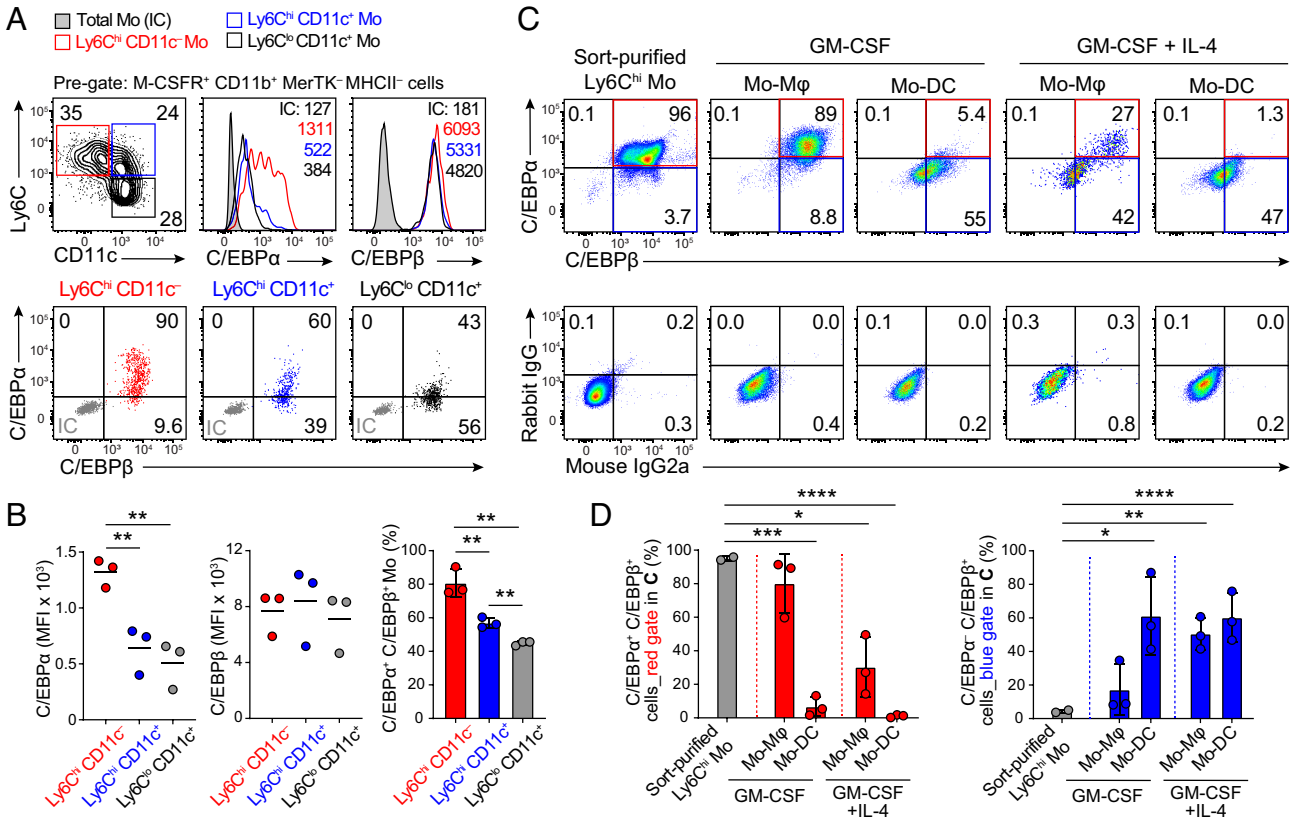

Fig. 2. Notch-induced Ly6C^{lo} monocytes extinguish C/EBPα expression. (*A*) Expression of C/EBPα and C/EBPβ was analyzed in monocytes differentiated from sort-purified cKit^{hi} BM progenitors with SCF, IL-3, and IL-6 conditioned media on OP9-DLL1 for 2 d. Pre-gate is CD45.2$^+$ CD115$^+$ CD11b$^+$ MerTK$^-$ MHCII$^-$ cells. Data shown is a representative of three similar experiments. IC denotes isotype control. (*B*) Scatter plots show average MFI of C/EBPα (*Left*) and C/EBPβ (*Middle*) in the cultured Ly6C^{hi} CD11c$^-$ (red), Ly6C^{hi} CD11c$^+$ (blue), and Ly6C^{lo} CD11c$^+$ (gray) monocytes. MFI shown is MFI of C/EBP-stained cell subtracted with MFI of isotype control. A bar-scatter graph (*Right*) exhibits percentages of C/EBPα$^+$ C/EBPβ$^+$ population in each monocyte of indicated (average % ±SD). (*C*) Expression of C/EBPα and C/EBPβ in sort-purified BM Ly6C^{hi} monocytes (*Left*), monocyte-derived macrophages and DCs cultured with 10 ng/mL GM-CSF (*Middle Left* two columns), or with 10 ng/mL GM-CSF plus 10 ng/mL IL-4 (*Right* two columns). (*D*) Bar-scatter graphs exhibit percentages of C/EBPα$^+$ C/EBPβ$^+$ population (*Left*, red) and C/EBPα$^-$ C/EBPβ$^+$ population (*Right*, blue) of the cultured cells as indicated. *P < 0.05, **P < 0.01, ***P < 0.001, ****P < 0.0001 (Student's t test).

studies (36) examined the impact of deleting approximately 1 kB surrounding the *Cebpa* +37 kb enhancer. Using CRISPR/Cas9 targeting, we deleted a 552 bp region to generate *Cebpa* +37$^{-/-}$ mice (*SI Appendix*, Fig. S2*A*). Mice homozygous for this deletion (*SI Appendix*, Fig. S2*B*) are viable and born at Mendelian frequencies. To verify the impact of our deletion, we examined C/EBPα protein expression in BM and splenic cells in *Cebpa* +37$^{-/-}$ mice using ICS (*SI Appendix*, Fig. S2*C*). We found severely reduced C/EBPα expression in both BM and spleen, consistent with previous studies (36, 37). In the liver, expression of C/EBPα by nonhematopoietic cells was unaffected in *Cebpa* +37$^{-/-}$ mice, indicating that this enhancer is not required for expression in this tissue (*SI Appendix*, Fig. S2*C*). We confirmed that our *Cebpa* +37$^{-/-}$ mice lack development of neutrophils in the spleen and blood (*SI Appendix*, Figs. S2*D* and S3 *A*–*F*), consistent with previous studies of the *Cebpa* +37 kb enhancer (36, 37). Of note, the BM progenitors and Ly6C^{lo} monocytes in the *Cebpa* +37$^{-/-}$ mice showed remarkably increased expression of C/EBPβ compared to the wild-type (WT) cells (*SI Appendix*, Fig. S2*E*).

***Cebpa* +37 kb Enhancer Is Required to Maintain Ly6C^{hi} Monocytes.** Previous analysis of the germline C/EBPα deficient mice identified a granulocyte defect but reported no changes in monocyte numbers (35). Subsequent analysis of *Cebpa* +37 kb enhancer mutants confirmed the previous neutrophil deficiency but claimed that monocytes were either slightly increased (36) or reported no changes in monocyte numbers (37). However, the analysis in these studies did not distinguish between Ly6C^{hi} monocytes and Ly6C^{lo} monocytes. Since we recently reported that BCL6 and IRF2 were additional requirements for Ly6C^{lo} monocytes (18), we wondered whether there might also be unrecognized requirements for the development of Ly6C^{hi} monocytes. Since C/EBPα was expressed selectively in Ly6C^{hi}, but not Ly6C^{lo} monocytes (Fig. 1), we paid particular attention to identifying Ly6C^{hi} and Ly6C^{lo} subsets in *Cebpa* +37$^{-/-}$ mice, (Fig. 3).

First, in BM, Ly6C^{hi} monocytes were markedly reduced in *Cebpa* +37$^{-/-}$ mice compared with WT controls (Fig. 3 *A* and *D* and *SI Appendix*, Fig. S3*G*). By contrast, Ly6C^{lo} monocytes were present, albeit with a slight reduction in their absolute numbers, attributed to a decrease in total BM cells in *Cebpa* +37$^{-/-}$ mice (*SI Appendix*, Fig. S3*G*). In the spleen, we also found that Ly6C^{hi} monocytes were dramatically reduced in *Cebpa* +37$^{-/-}$ mice compared with WT controls (Fig. 3 *B* and *D* and *SI Appendix*, Fig. S3*H*). Again, Ly6C^{lo} monocytes were present with a slight decrease in their absolute number by comparison to Ly6C^{hi} monocytes (*SI Appendix*, Fig. S3*H*). A small population was apparent in Ly6C^{hi} monocytes but was reduced by approximately 10-fold in percentage and 40-fold in the absolute number compared with WT control mice (Fig. 3*D* and *SI Appendix*, Fig. S3*H*). Finally, in blood, Ly6C^{hi} monocytes were reduced in *Cebpa* +37$^{-/-}$ mice compared with WT controls (Fig. 3 *C* and *D*). In contrast to Ly6C^{hi} monocytes, we find no significant reduction in Ly6C^{lo} monocytes by the percentage in the BM, spleen, and blood of *Cebpa* +37$^{-/-}$ mice (Fig. 3 *A*–*D*). The transcriptional profile of Ly6C^{lo} monocytes from WT and *Cebpa* +37$^{-/-}$ mice was

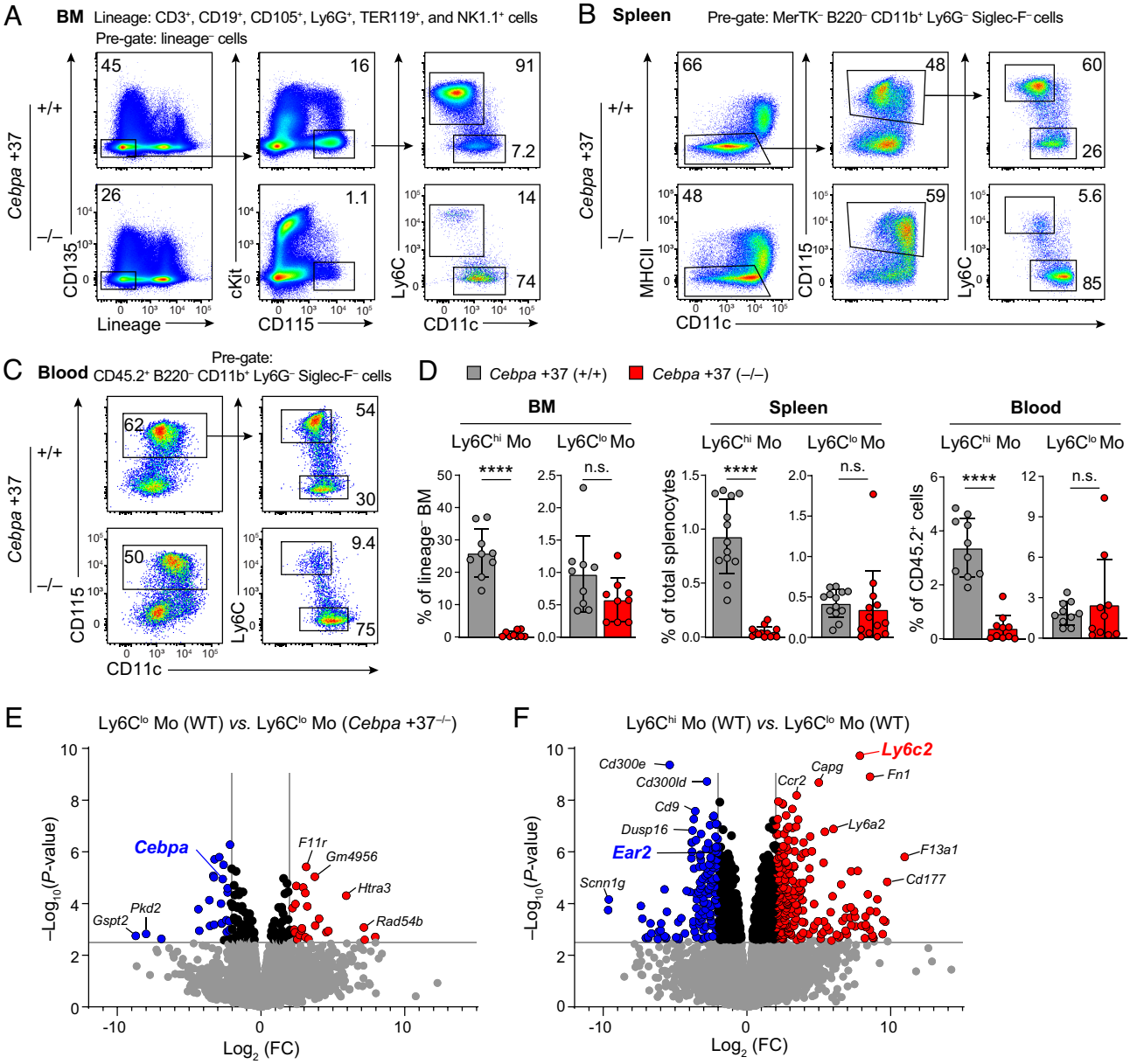

Fig. 3. Development of Ly6C^{hi} monocytes requires the *Cebpa* +37 kb enhancer. (*A*–*C*) Flow cytometric analysis showing monocytes in the (*A*) BM, (*B*) spleen, and (*C*) peripheral blood in the WT (*Cebpa* +37$^{+/+}$) and *Cebpa* +37$^{-/-}$ mice. (*D*) Bar-scatter plots show frequencies of Ly6C^{hi} monocytes and Ly6C^{lo} monocytes in the indicated tissues of WT (gray) and *Cebpa* +37$^{-/-}$ mice (red), (average % ±SD). Individual mice are indicated as dots (n = 9, each). ****P < 0.0001 (Student's t test). n.s. denotes "not significant." (*E* and *F*) RNA-seq performed on monocytes sort-purified from WT and *Cebpa* +37$^{-/-}$ spleen. Volcano plots show differentially expressed genes as the fold-change (FC) (*E*) between splenic Ly6C^{lo} monocytes isolated from WT and *Cebpa* +37$^{-/-}$ mice and (*F*) between Ly6C^{hi} monocytes and Ly6C^{lo} monocytes obtained from the WT spleen. Differentially expressed genes with >fourfold changes are highlighted in red (increased) or blue (decreased).

very similar, showing only 57 differentially expressed genes with >fourfold changes (>–$\log_{10}$ P-value 2.5) which primarily included genes expressed by tissue macrophages such as *F11r*, *Htra3*, and *Rad54b*, upon *Cebpa* deficiency (Fig. 3*E*). In contrast, the transcriptional profile of Ly6C^{hi} and Ly6C^{lo} monocytes from WT mice were substantially different, showing 365 differentially expressed genes with >fourfold change (>–$\log_{10}$ P-value 2.5) (Fig. 3*F*). Unlike RNA isolation from most myeloid cells, isolating high-quality RNA from Ly6C^{lo} monocytes required addition of a RNase inhibitor, which may be the results of their high level of *Ear2* (*Rnase2*) expression compared to Ly6C^{hi} monocytes (Fig. 3*F*). Finally, cDC development appeared normal in *Cebpa* +37$^{-/-}$ mice (*SI Appendix*, Fig. S3 *I* and *J*). In summary, *Cebpa* +37$^{-/-}$ mice have a substantial and selective reduction in Ly6C^{hi} monocytes while having persistence of the Ly6C^{lo} monocyte population.

***Cebpa* +37$^{-/-}$ BM Lack cMoP to Generate Ly6C^{lo} Monocytes.** Previous analysis of BM from *Cebpa* +37$^{-/-}$ mice showed a reduction in the GMP (36, 37). However, neither study of the *Cebpa* +37 kb enhancer mutants noted the absence of the cMoP (36, 37). Since Ly6C^{hi} monocytes are absent in *Cebpa* +37$^{-/-}$ mice, we next examined BM to identify other potential changes in monocyte development (Fig. 4) including the MDP, GMP, and cMoP.

We first compared BM from WT and *Cebpa* +37$^{-/-}$ mice for the development of the cMoP. The cMoP was originally defined as Lin$^-$ cKit$^+$ CD115$^+$ CD135$^-$ Ly6C^{hi} CD11b$^-$ BM cells (5) (Fig. 4*A*). Using this definition, *Cebpa* +37$^{-/-}$ mice show a dramatic reduction in the cMoP population. The cMoP was initially defined as a cKit^{hi} population (5). By this criterion, the cMoP is absent in *Cebpa* +37$^{-/-}$ mice (Fig. 4*A*), based primarily on the lack of Ly6C expression in Lin$^-$ cKit^{hi} CD115$^+$ CD135$^-$ BM cells. However, we

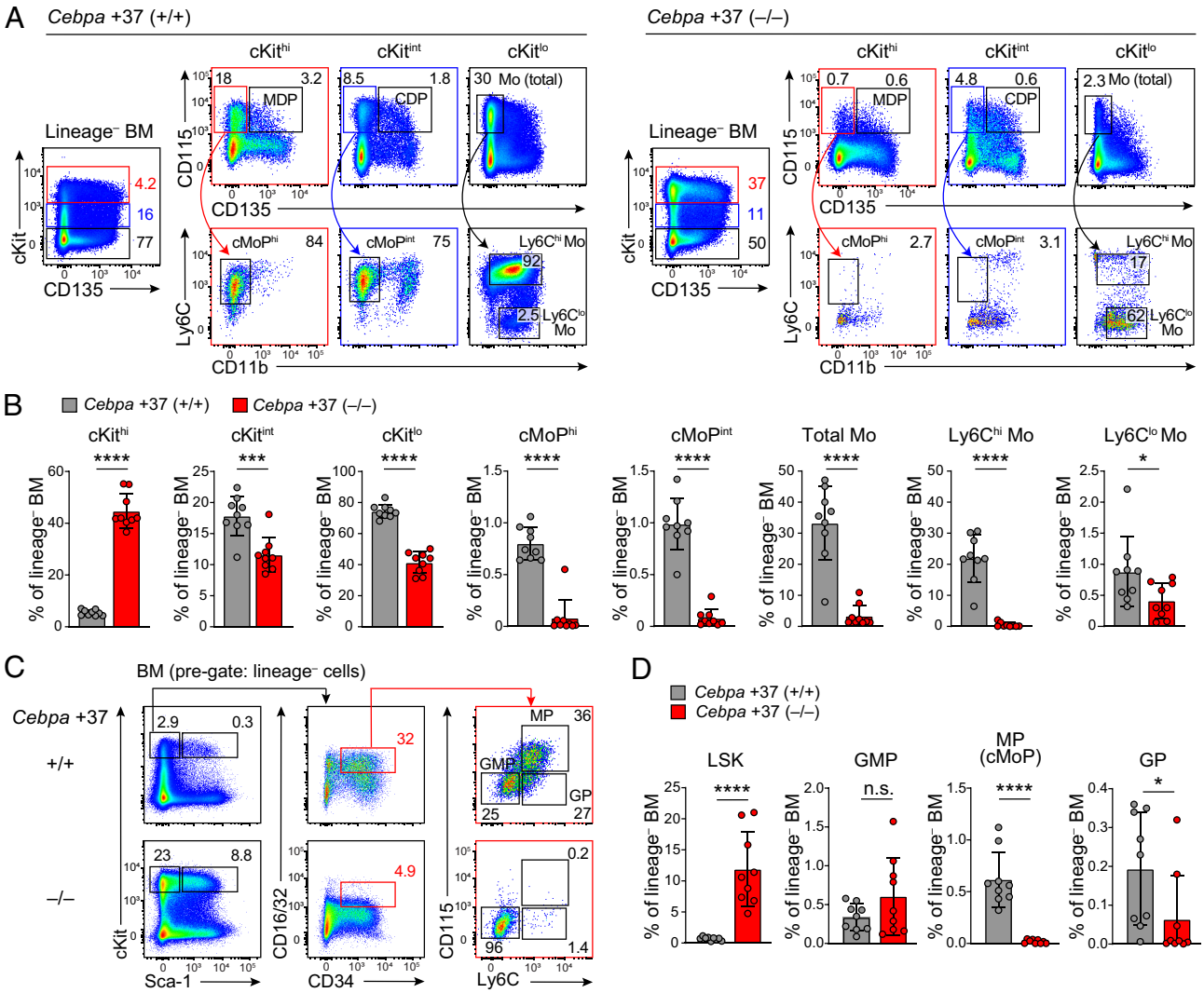

Fig. 4. Committed monocyte progenitors are severely reduced in *Cebpa* +37$^{-/-}$ mice. (*A*) Flow cytometric analysis show BM progenitors and monocytes in the WT and *Cebpa* +37$^{-/-}$ mice. Development of cMoP and MDP in the cKit^{hi} BM cells (red), cMoP and CDP in the cKit^{int} BM cells (blue), and monocytes in the cKit^{lo} BM cells (black) in the WT (*Left Upper*) and *Cebpa* +37$^{-/-}$ mice (*Right Upper*). Ly6C and CD11b expression of cMoP and monocyte populations was shown on the *Lower* panels of each genotype. (*B*) Bar-scatter plots show frequencies of BM progenitors shown in (*A*) in the lineage$^-$ BM cells (average % ±SD). Lineage-committed population is comprised of CD3ε$^+$ CD19$^+$ CD105$^+$ Ly6G$^+$ TER119$^+$, or NK1.1$^+$ cells. (*C*) Development of LSK, GMP, MP (cMoP), and GP in the WT (*Upper*) and *Cebpa* +37$^{-/-}$ mice (*Lower*). (*D*) Bar-scatter graphs show frequencies of LSK, GMP, MP (cMoP), and GP in the lineage$^-$ BM cells (average % ±SD). *P < 0.05, ***P < 0.001, ****P < 0.0001 (Student's t test). n.s. denotes "not significant."

observed partial and transient Ly6C expression in Kit^{int} CD115$^+$ CD135$^-$ progenitors, which also express CD11b (Fig. 4*A*). In WT mice, Lin$^-$ CD115$^+$ CD135$^-$ BM cells in both cKit^{hi} and cKit^{int} populations are uniformly positive for Ly6C expression. By contrast, in *Cebpa* +37$^{-/-}$ mice, only a small fraction of cKit^{int} CD115$^+$ CD135$^-$ BM cells express Ly6C, suggesting either delayed or transient Ly6C expression in the absence of C/EBPα.

We next compared BM from WT and *Cebpa* +37$^{-/-}$ mice for development of the GMP. The GMP in WT was originally defined as Lin$^-$ cKit$^+$ Sca-1$^-$ CD16/32$^+$ CD34$^+$ BM cells (39), and recently modified as being CD115$^-$ Ly6C^{lo} (10, 40). Using the original definition, the GMP is reduced in *Cebpa* +37$^{-/-}$ mice primarily due to lower CD16/32 expression on cKit$^+$ Sca-1$^-$ BM cells (Fig. 4*C*), in agreement with the original study of *Cebpa*$^{-/-}$ mice (36). The GMP was subsequently recognized to contain a specified CD115$^-$ Ly6C^{hi} granulocyte progenitor (GP) and CD115$^+$ Ly6C^{hi} monocyte progenitor, called MP (40) and cMoP (10) respectively. Using these definitions, both GPs and cMoPs are absent in *Cebpa* +37$^{-/-}$ mice (Fig. 4 *C* and *D*). Additionally, no developmental defects in either MDP or CDP were observed in *Cebpa* +37$^{-/-}$ BM (Fig. 4*A* and *SI Appendix*, Fig. S3*K*), suggesting that the MDP may be the source of Ly6C^{lo} monocytes in *Cebpa* +37$^{-/-}$ mice (Fig. 5).

***Cebpa* +37$^{-/-}$ BM Progenitors Spontaneously Bypass the cMoP to Generate Ly6C^{lo} Monocytes.** The above results suggest that progenitors in *Cebpa* +37$^{-/-}$ mice progress from either the MDP (Fig. 4*A*) or a Lin$^-$ Sca1$^-$ cKit^{hi} CD16/32^{lo} progenitor (Fig. 4*C*) and bypass the cMoP to directly generate Ly6C^{lo} monocytes. To test this, we examined the behavior of BM progenitors in WT and *Cebpa* +37$^{-/-}$ mice in culture (Fig. 6). First, we cultured purified cKit^{hi} BM progenitors from WT and in *Cebpa* +37$^{-/-}$ mice in vitro with SCF, IL-3 and IL-6 as previously described (18, 37). In these cultures, WT progenitors generate Ly6G$^+$ neutrophils and Ly6C^{hi} monocytes (Fig. 6*A*). Importantly, virtually no Ly6C^{lo} monocytes develop (Fig. 6*A*), consistent with the absence of Notch signaling in this culture system (*SI Appendix*, Fig. S1*E*). By contrast, *Cebpa* +37$^{-/-}$ progenitors fail to generate neutrophils, as expected but also fail to generate Ly6C^{hi} monocytes, and instead generate predominantly Ly6C^{lo} CD11c$^+$ monocytes (Fig. 6 *A* and *B*). These results confirm our in vivo finding and suggest that C/EBPα acts

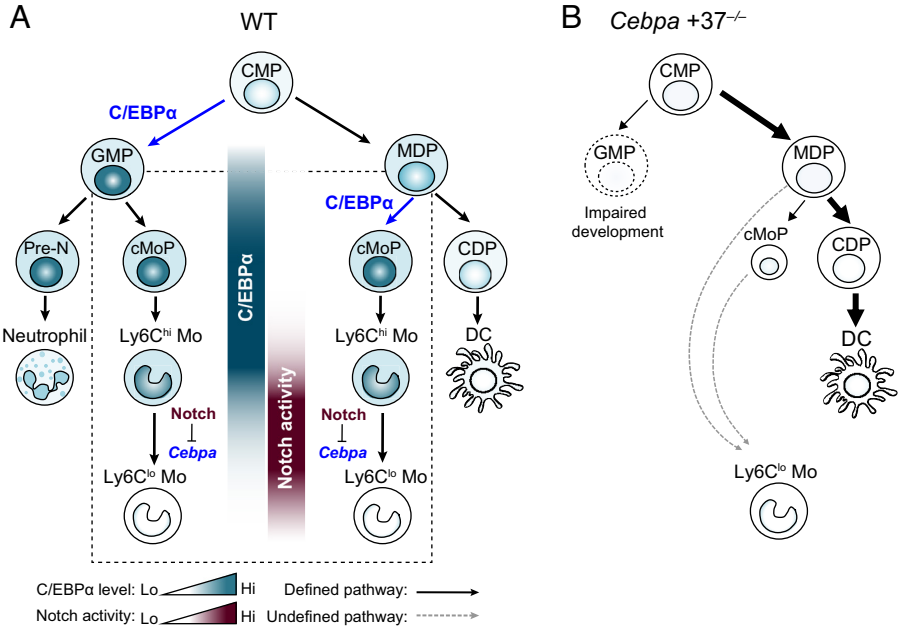

Fig. 5. Monocyte development under normal and *Cebpa*-deficient conditions. (*A*) Under the normal condition (WT), both GMP and MDP develop into cMoP, which further gives rise to both Ly6C^{hi} monocytes and Ly6C^{lo} monocytes. C/EBPα controls the transition of common myeloid progenitor (CMP) to GMP and the transition of MDP to cMoP. Downregulation of C/EBPα expression upon activation of Notch signaling promotes Ly6C^{hi} monocytes develop into Ly6C^{lo} monocytes. (*B*) *Cebpa* +37$^{-/-}$ BM exhibits a significant loss of GMP, thus MDP may be the main source of cMoP and Ly6C^{lo} monocytes under the *Cebpa*-deficient condition. The intensities of the teal color in the nucleus of each cell diagram reflect the levels of C/EBPα, white or weak teal indicating lower expression and strong teal indicating higher expression. The solid black arrow and dotted gray arrow indicate the defined and undefined developmental pathways of BM progenitors for myeloid lineages, respectively.

to maintain Ly6C^{hi} monocyte identity by halting their progression to Ly6C^{lo} monocytes.

WT cKit^{hi} BM progenitors cultured in SCF, IL-3, and IL-6 do not produce cDCs (Fig. 6 *A* and *B*). Surprisingly, *Cebpa* +37$^{-/-}$ progenitors generated cDCs with strikingly increased frequency (Fig. 6 *A* and *B*). In addition, these results suggest that C/EBPα may regulate MDP divergence, favoring cMoP development at the expense of CDPs.

We next asked whether C/EBPα acts to support Ly6C expression directly or alternately functions more broadly to maintain Ly6C^{hi} monocyte identity. We noticed that *Cebpa* +37$^{-/-}$ mice have a small population of neutrophil-like cells expressing Ly6G (*SI Appendix,* Fig. S3 *A* and *C*). In these cells, we found that Ly6C expression was maintained at levels similar to WT neutrophils (*SI Appendix,* Fig. S3 *B* and *D*). This suggests that Ly6C itself can be expressed without *Cebpa*, which may favor a role for *Cebpa* in maintaining Ly6C^{hi} monocyte identity. Since neutrophils do not express C/EBPα (*SI Appendix,* Fig. S2*D*), Ly6C may also be controlled by additional factors.

Differential translation of *Cebpa* mRNA produces a 42 kDa long C/EBPα isoform (p42) and a 30 kDa short C/EBPα isoform (p30) (41, 42). We asked how these C/EBPα isoforms functioned in support of Ly6C^{hi} monocyte development. We expressed p42 and p30 C/EBPα isoforms by retrovirus into cKit^{hi} progenitors from WT or *Cebpa* +37$^{-/-}$ mice (Fig. 6 *C* and *D*). In WT progenitors, which support only Ly6C^{hi} monocyte development in this culture, expression of p42 caused a moderate reduction in CD115^{+} monocyte development, while p30 had little effect (Fig. 6*C*). However, in *Cebpa* +37$^{-/-}$ progenitors, which develop only into Ly6C^{lo} monocytes, p30 strongly restored Ly6C^{hi} monocyte development (Fig. 6 *C* and *D*). The p42 isoform was substantially weaker compared to p30 in restoring Ly6C^{hi} monocyte development (Fig. 6 *C* and *D*). Notably, both p42 and p30 strongly repressed cDC development from *Cebpa* +37$^{-/-}$ progenitors. These results, in some agreement with a recent study (43), suggest that C/EBPα isoforms act differently in MDP divergence vs. maintaining Ly6C^{hi} monocyte identity.

***Cebpa* +37$^{-/-}$ Mice Have Altered the Development of Monocyte-Derived Peritoneal Macrophages.** Most tissue-resident macrophages originate from embryonic progenitors (44) but can be replaced by HSC-derived monocytes over time under homeostatic and inflammatory conditions (45–47). A population of peritoneal macrophages expressing CD226 and MHC class II (MHCII) has been reported to arise from circulating monocytes after birth (48). We asked whether these CD226^{+} MHCII^{+} peritoneal macrophages develop in *Cebpa* +37$^{-/-}$ mice (*SI Appendix,* Fig. S4). First, CD226^{+} MHCII^{+} peritoneal macrophages were reduced in *Cebpa* +37$^{-/-}$ mice compared to WT mice (*SI Appendix,* Fig. S4 *A* and *B*). In WT mice, CD226^{+} MHCII^{+} peritoneal macrophages comprised both CD11c^{-} and CD11c^{+} fractions (*SI Appendix,* Fig. S4 *A* and *B*) similar to previous analysis (48). In contrast, in *Cebpa* +37$^{-/-}$ mice, CD226^{+} MHCII^{+} peritoneal macrophages were primarily CD11c-expressing cells (*SI Appendix,* Fig. S4 *A* and *B*).

Previous studies suggested that CD226^{+} peritoneal cells may be MoDCs (49, 50). However, the distinction between CD226^{+} MoDCs and CD226^{+} MHCII^{+} peritoneal macrophages is unclear. We examined CD226^{+} MHCII^{+} peritoneal cells in *Zbtb46*^{egfp} reporter mice (*SI Appendix,* Fig. S4*C*). CD226^{+} MHCII^{+} peritoneal cells appeared heterogeneous for CD11c in *Zbtb46*^{egfp} mice, similar to WT mice. However, CD11c^{lo} CD226^{+} MHCII^{+} peritoneal cells also expressed low levels of *Zbtb46*-EGFP, while CD11c^{hi} CD226^{+} MHCII^{+} peritoneal cells expressed high levels of *Zbtb46*-EGFP (*SI Appendix,* Fig. S4*D*). These results suggest that C/EBPα may regulate the transition of *Zbtb46*^{lo} CD11c^{lo} CD226^{+} MHCII^{+} peritoneal cells to *Zbtb46*^{hi} CD11c^{hi} CD226^{+} MHCII^{+} peritoneal cells, similar to its regulation of the Ly6C^{hi} to Ly6C^{lo} monocyte transition.

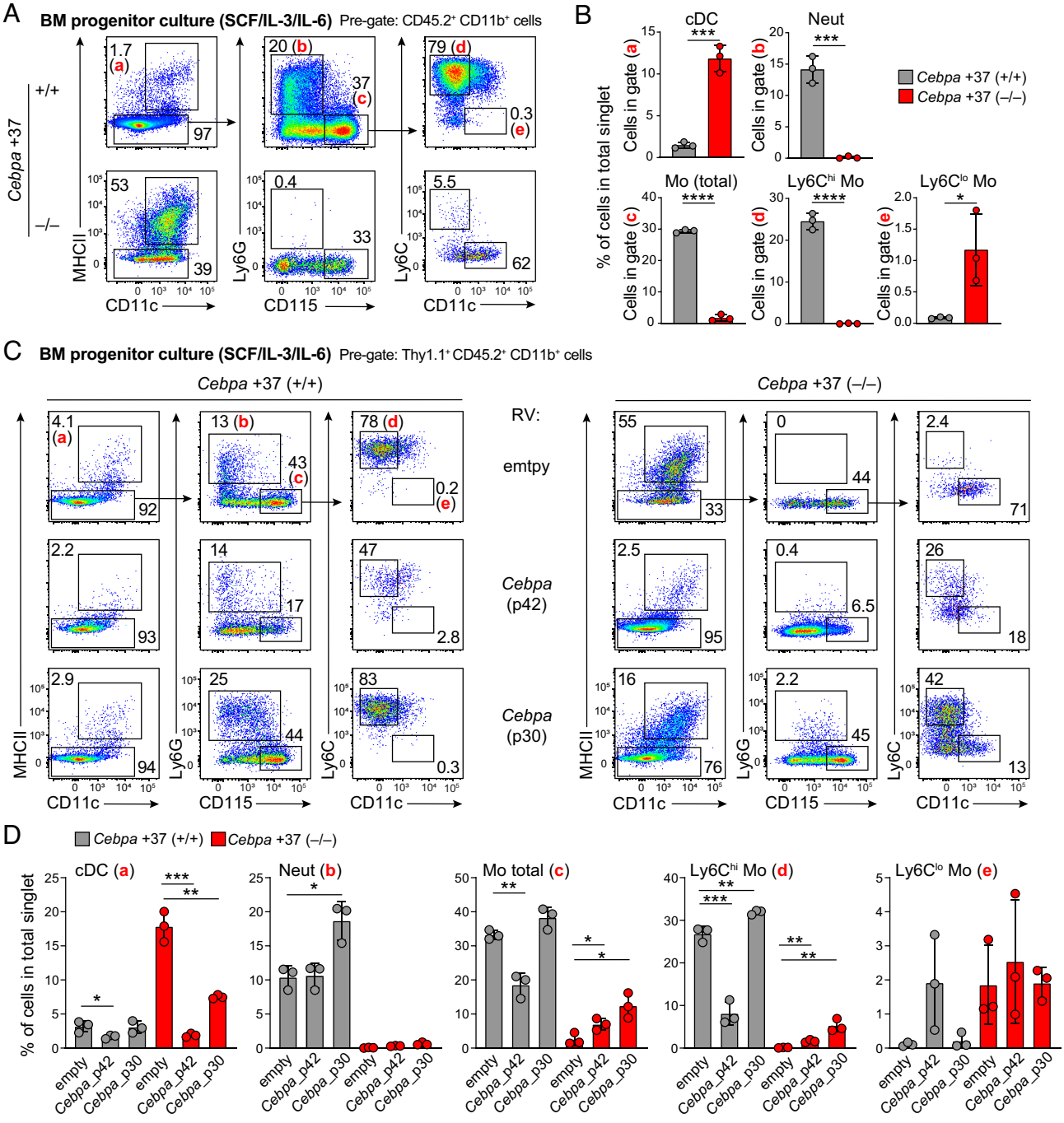

Fig. 6. *Cebpa* +37$^{-/-}$ BM progenitors differentiate directly into Ly6C^{lo} monocytes. (*A–D*) Sort-purified cKit^{hi} BM progenitors from WT (*Cebpa* +37$^{+/+}$) and *Cebpa* +37$^{-/-}$ mice were cultured with conditioned media containing SCF, IL-3, and IL-6 for 60 h. (*A*) Flow cytometric analysis showing cell populations in the WT (*Upper*) and *Cebpa* +37$^{-/-}$ cells (*Lower*). Pre-gate is CD45.2^{+} CD11b^{+} cells. MHCII^{+} CD11c^{+} cells are cDC gated as "a." MHCII^{-} Ly6G^{+} CD115^{-}cells are neutrophils (Neut) gated as "b." MHCII^{-} Ly6G^{-} CD115^{+} cells are monocytes (Mo) gated as "c." Ly6C^{hi} monocytes (Ly6C^{hi} Mo) and Ly6C^{lo} monocytes (Ly6C^{lo} Mo) are gated as "d" and "e," respectively. (*B*) Bar-scatter graphs show frequencies of each cell population (gate "a" to "e") of WT (gray) and *Cebpa* +37$^{-/-}$ cells (red) in total singlet (average % ±SD). (*C*) Retroviral (RV) overexpression of *Cebpa* full-length (p42) and truncated (p30) isoforms in the WT and *Cebpa* +37$^{-/-}$ cKit^{hi} BM progenitors. Pre-gate is Thy1.1^{+} (marker for RV-infected cells) CD45.2^{+} CD11b^{+} cells. Refer to (*A*) for cell populations gated as "a" to "e." (*D*) Bar-scatter graphs show frequencies of each cell population (gates "a" to "e") of WT (gray) and *Cebpa* +37$^{-/-}$ cells (red) transduced with empty (control RV), *Cebpa*_p42-RV, and *Cebpa*_p30-RV in the total singlet (average % ±SD). Data shown (*A* and *C*) is a representative of three same experiments. **P* < 0.05, ***P* < 0.01, ****P* < 0.001, *****P* < 0.0001 (Student's *t* test).

Discussion

Here, we report a previously unrecognized requirement for C/EBPα in monocyte development. Several previous studies examined the impact of C/EBPα deficiency on hematopoietic lineages using either germline inactivation (35, 51) or deletion of the *Cebpa* +37 kb enhancer (36, 37). Each study identified severe reduction of neutrophil, eosinophils, and tissue macrophages but none reported an impact on monocytes (35–37, 51). Despite longstanding recognition of human monocyte heterogeneity (52–58), the first study of *Cebpa* deficiency (35) was performed before monocyte heterogeneity was well characterized in mice (2, 59–61). That study examined monocytes by histological appearance and described no change caused by C/EBPα deficiency. Two subsequent studies of mice with deletions of the *Cebpa* +37 kb enhancer did analyze monocytes by FACS, but only used CD11b (Mac-1) or Ly6C/Ly6G

(Gr-1) as markers (36, 37) but did not use Ly6C (2), TREML4, or CD11c (61) that can distinguish between Ly6C^{hi} and Ly6C^{lo} monocytes.

Prior studies document roles for C/EBPα in neutrophil and macrophage development but did not demonstrate its role in maintaining Ly6C^{hi} monocytes. First, inducible C/EBPα expression potentiated myeloid gene expression in bone marrow cells by increasing the expression of PU.1 (62). Cooperative binding of C/EBPα and PU.1 activated enhancers for myeloid genes, redirecting the fate of pre-B cell toward macrophages (63), suggesting that C/EBPα may impact monopoiesis. Finally, *Cebpa*$^{-/-}$ BM failed to support the recovery of peritoneal macrophage after thioglycollate treatment (51), which is normally supported by circulating monocytes (10), but this study did not identify a defect in monocytes.

Our finding enhances the understanding of the Ly6C^{hi} to Ly6C^{lo} monocyte transition (Fig. 5). Prior findings that Notch2 signaling triggers Ly6C^{hi} monocytes to transition into Ly6C^{lo} monocytes have been explained on a mechanistic basis (16). Our results identify the first factor to selectively maintain Ly6C^{hi} monocytes, and suggest a potential relationship to Notch signaling (Fig. 5). Several other transcription factors are known to regulate monocyte development. PU.1 deficiency causes broad defects in lymphoid and myeloid lineages (25). Deficiencies in IRF8 and KLF4 also impair both Ly6C^{hi} and Ly6C^{lo} monocytes (26, 29), while deficiencies in C/EBPβ, NUR77, BCL6, and IRF2 selectively impair Ly6C^{lo} monocyte development (18, 20). Thus, few candidates are available to mediate Notch-induced transition of Ly6C^{hi} monocytes into Ly6C^{lo} monocytes.

NUR77 and C/EBPβ are increased during the Ly6C^{hi} to Ly6C^{lo} monocyte transition (18) and are required for Ly6C^{lo} monocytes (4, 20). We find that C/EBPβ cannot substitute for C/EBPα in the development of neutrophils or Ly6C^{hi} monocytes (*SI Appendix*, Fig. S2*E*), despite the previous suggestion that these factors may be functionally redundant in vivo (64–67). We recently reported two additional transcriptional requirements for Ly6C^{lo} monocyte development, BCL6 and IRF2 (18). BCL6 expression increases during the Ly6C^{hi} to Ly6C^{lo} monocyte transition (18). Additional studies are required to determine the relationship between all these factors and Notch signaling.

Finally, we observed differences in the effect of C/EBPα isoforms in restoring monocyte and neutrophil development. P30 expression in *Cebpa* +37$^{-/-}$ BM progenitors restored Ly6C^{hi} monocytes, but p42 suppressed total monocyte development. While this could result from interactions with distinct factors, different DNA binding motifs have also been reported for p42 and p30 (43), with p42 showing motifs for HLF, TEF, and CEBP, while p30 showed motifs for Ets family transcription factors such as PU.1 and ETVs (43). However, evidence of cooperative binding with these factors has not been reported. Additional studies will be required to establish the differential actions of C/EBPα isoforms in neutrophil and monocyte development.

Materials and Methods

Generation of *Cebpa* +37 kb Enhancer Deletion Mouse. Enhancer deletion mice were generated as previously described (68). sgRNAs flanking the *Cebpa* +37 kb enhancer were identified using CRISPR Guide RNA Design Tool from Benchling (https://benchling.com/crispr). The following single guide (sg) RNA sequences were used:

5′-AGGGCAATTTCAGCCCCAAG (*Cebpa* +37 kb sgRNA1);

5′-ACGTAGACCCTCTCCTGACA (*Cebpa* +37 kb sgRNA2). Each sgRNA oligonucleotide, Cas9 nuclease, and nuclease-free duplex buffer were purchased from Integrated DNA Technologies. Ribonucleoprotein (RNP) complex for each sgRNA was separately generated. Briefly, 200 pmol of each sgRNA was mixed with 50 pmol Cas9 nuclease in 25 μL of nuclease-free duplex buffer in separate microtubes, incubated 15 min at room temperature. Microinjection was performed at Transgenic, Knockout, and Micro-Injection Core at Washington University in St. Louis as previously reported (68). Briefly, single-cell zygotes isolated from C57BL/6 mice on day 0.5 were injected with 8 mM RNP complex by electroporation. The RNP-electroporated zygotes were transferred into the oviducts of pseudopregnant recipient mice.

Targeted mosaic mice were screened by PCR using following primers:

Cebpa +37 kb forward: 5′-CCCAAGACAGCCAGGTTAGG;

Cebpa +37 kb reverse: 5′-GGTGCTCCTGGGTTAATGGCT.

Cebpa +37 kb reverse specific for WT: 5′-ACACTTCACCCTCTTGGGGC.

Targeted mice were outcrossed to wild-type (WT) C57BL6/J mice (JAX:000664), and the resulting heterozygous mice were intercrossed to generate homozygous *Cebpa* +37 kb deletion mice. *Zbtb46*^{egfp} reporter mice were previously reported (69) and kept in house. All mice were maintained in a specific pathogen-free animal facility following institutional guidelines with protocols approved by Animal Studies Committee at Washington University in St. Louis. Most of experiments were performed with mice between 6 and 12 wk of age.

Flow Cytometric Analysis and Sorting. BM progenitor cells and splenocytes were purified and stained as previously described (18, 70, 71). All procedures for cell staining were performed in PBS supplemented with 2 % of FBS and 2 mM EDTA (MACS buffer). Lineage (Lin)-committed cells in the BM were defined as CD3ε$^+$, CD19$^+$, CD105$^+$, Ly6G$^+$, TER119$^+$, or NK1.1$^+$ cells. BM progenitors were defined as follows: LSK as Lin$^-$ Sca-1$^+$ cKit^{hi} cells, GMP as Lin$^-$ Sca-1$^-$ cKit^{hi} CD16/32$^+$ CD34$^+$ Ly6C$^-$ CD115$^-$ cells, GP as Lin$^-$ Sca-1$^-$ cKit^{hi} CD16/32$^+$ CD34$^+$ Ly6C$^+$ CD115$^-$ cells, MP as Lin$^-$ Sca-1$^-$ cKit^{hi} CD16/32$^+$ CD34$^+$ Ly6C$^-$ CD115$^+$ cells, MDP as Lin$^-$ cKit^{hi} CD135$^+$ CD115$^+$ cells, and cMoP as Lin$^-$ cKit^{hi} CD135$^-$ CD115$^+$ Ly6C$^+$ CD11b$^-$ cells. Cells were stained as previously described for sorting and analysis (18, 70, 71). Biotinylated antibodies used for Lin-committed cells for BM progenitor analysis are as follows: anti-mouse CD3ε (clone 145-2C11), CD19 (clone 6D5), Ly6G (clone 1A8), TER119 (clone TER-119), and NK1.1 (clone PK136) antibodies were purchased from BioLegend. Anti-mouse CD105 antibody (clone MJ7/18) was obtained from Invitrogen. Fluorochrome-conjugated antibodies for cell staining are as follows: anti-mouse Siglec-H (PE, clone 551), I-A/I-E (BV510, clone M5/114.15.2, for MHC class II), Sirp-α (APC, clone P84), Ly6G (FITC, clone 1A8), CD34 (PE, clone SA376A4), CD226 (PE, clone 10E5), XCR1 (BV421, clone ZET), CD11b (AF647 or APC, clone M1/70), CD115 (BV711, clone AFS98), Ly6C (BV421, clone HK1.4), CD45.2 (PE-Cy7, clone 104), Ly6A/E (PE-Cy7, clone E13-161.7, for Sca-1), CD45R/B220 (AF488, clone RA3-6B2), F4/80 (APC-Cy7, clone BM8), and CD11c (AF647, clone N418) antibodies were obtained from BioLegend. Anti-mouse CD45R/B220 (BUV395, clone RA3-6B2), CD90.1/Thy1.1 (BUV395, clone OX-7), cKit (BUV395, clone 2B8), CD135 (PE-CF594, clone A2F10.1), CD45.2 (BV786, clone 104), Ly6G (PE, clone 1A8), CD11b (PE-Cy7, clone M1/70), and Siglec-F (PE, clone E50-2440) antibodies were purchased from BD Biosciences. Anti-mouse MerTK (PE-Cy7, clone DS5MMER), CD16/32 (APC, clone 93), and CD11c (APC-ef780, clone N418) antibodies were purchased from eBioscience™. Anti-human/mouse CD11b (FITC, clone M1/70) antibody was purchased from TONBO biosciences. BV785™ Streptavidin was obtained from BioLegend. Antibodies used for intracellular staining of C/EBPα and C/EBPβ are as follows: Anti-human/mouse C/EBPα (clone D56F10) and anti-mouse C/EBPβ (clone H-7) antibodies were purchased from Cell Signaling Technology and Santa Cruz, respectively. Normal rabbit IgG and mouse IgG2a (HOPC-1), used as isotype controls for C/EBPα and C/EBPβ staining, were from MilliporeSigma and SouthernBiotech, respectively. Donkey anti-rabbit IgG (FITC) and goat anti-mouse IgG2a (R-PE) antibodies were purchased from Jackson ImmunoResearch and used as secondary antibodies. Cells were analyzed on a FACSAria Fusion flow cytometer (BD Biosciences), and data were analyzed with FlowJo v10 software (TreeStar).

Intracellular Staining. BM progenitors, splenocytes, and peripheral blood cells were isolated as previously described (70, 71). Briefly, cell surface staining was performed to identify monocytes and their progenitors. The cells were suspended in 400 μL 1× Fixation/Permeabilization buffer (Invitrogen, 005123-43 and 00-5223-56), incubated for 30 min at room temperature, and then washed with 400 μL 1X Permeabilization buffer (Invitrogen, 00-8333-56) twice. The fixed cells (~10^7 cells) were resuspended in 50 μL 1× Permeabilization buffer containing

C/EBPα (final concentration 207 ng/mL) and C/EBPβ (final concentration 4 μg/mL) antibodies, or isotype control antibodies (207 ng/mL rabbit IgG for C/EBPα and 4 μg/mL mouse IgG2a for C/EBPβ antibodies), then incubated at room temperature, overnight at dark. After washing with 400 μL 1× Permeabilization buffer, the cells were incubated with 50 μL 1× Permeabilization buffer containing FITC-conjugated anti-rabbit IgG and PE-conjugated anti-mouse IgG2a antibodies for 30 min, at room temperature. Cells were washed with MACS buffer and analyzed by flow cytometer.

In Vitro Cell Culture. Lin^- $cKit^{hi}$ BM progenitor cells were sort-purified from WT or *Cebpa* $+37^{-/-}$ mice. Then, 1.5 to 2.5 × 10^4 cells were seeded in a 96-well cell culture plate (flat bottom) and cultured with conditioned media containing SCF, IL-3, and IL-6 (5%, each), for 2 d. To differentiate $Ly6C^{hi}$ and $Ly6C^{lo}$ monocytes in vitro, 2.5 × 10^4 Lin^- $cKit^{hi}$ BM progenitor cells were cultured with 2.5 × 10^4 of OP9-DLL1 or OP9 cells, for 2 d. To differentiate monocyte-derived DCs and macrophages, 1.5 to 2.0 × 10^5 sort-purified BM $Ly6C^{hi}$ monocytes were cultured with murine recombinant GM-CSF (10 ng/mL, Peperotech) combined with or without murine recombinant IL-4 (10 ng/mL, Peprotech) for 5 d. Iscove's modified Dulbecco's medium (IMDM, Gibco, Thermo Fisher Scientific) supplemented with 10% FBS (cytiva, HyClone), 1% penicillin-streptomycin solution (Gibco, Thermo Fisher Scientific), 1% MEM nonessential amino acid (Gibco, Thermo Fisher Scientific), 1% L-glutamine solution (Gibco, Thermo Fisher Scientific), 1% sodium pyruvate (Corning®), and 55 μM β-mercaptoethanol (Sigma-Aldrich) was used for cell culture.

RNA-Seq. $Ly6C^{hi}$ monocytes and $Ly6C^{lo}$ monocytes (approximately 40,000 to 50,000 cells/sample) were sorted from WT or *Cebpa* $+37^{-/-}$ splenocytes and collected into 100 μL MACS buffer containing 40 U of Protector RNase inhibitor (Roche) to prevent RNA degradation. The procedures for RNA-seq analysis including library generation, sequencing, and alignment were previously described (72).

Peritoneal Lavage for Macrophage Analysis. Mice killed with CO_2 were injected with 3 mL MACS buffer using a 5-mL syringe (BD Luer-Lok™) with 25G × 5/8 in a needle (BD PrecisionGlide™). The abdomen of the mice was massaged 10 times with fingers, then 2 mL of the peritoneal fluid was collected. Ammonium-chloride-potassium (ACK) buffer was used to remove red blood cells as needed. A million cells were stained and analyzed by flow cytometer.

Plasmids, Retroviral Packaging, and Overexpression. *Cebpa* p42 and p30 were amplified from cDNA of *Cebpa* (pcDNA3 Flag C/EBPα was a gift from Christopher Vakoc (Addgene plasmid # 66978; https://n2t.net/addgene:66978; RRID:Addgene_66978) (73) using forward p42 primer (catagatctGCCACCATGGAGTCGGCCGACTTCT), forward p30 primer (5′-tatagatctGCCACCATGTCCGCGGGGGCGCA) and common reverse primer (5′-aatactcgagCGCGCAGTTGCCCATGGC), and cloned as a BglII/XhoI fragment into MSCV-based retroviral vector (T2a-Thy1.1 RV) (72) to generated MSCV-p42-T2a-Thy1.1 and MSCV-p30-T2a-Thy1.1. Restriction enzyme sites for BglII or XhoI in the primers were indicated with a single underline. Double underlined "GCCACC" is Kozak sequence. Retroviral constructs were packaged using Plat-E cells transfected with TransIT (Mirus bio) as described (70).

Cell Lines. Packaging cell line, Platinum-E (Plat-E) (74), for generation of retrovirus was cultured in complete IMDM. 0.25% Trypsin-EDTA (Gibco, Thermo Fisher Scientific) was used for cell passaging.

Statistics. All bar-scatter plots with error bars and statistical analyses were performed with GraphPad Software (Prism version 10).

Data, Materials, and Software Availability. The RNA-seq data are available on the Gene Expression Omnibus (GEO) database with the accession number GSE254202 (75). All other data are included in the manuscript and/or *SI Appendix*.

ACKNOWLEDGMENTS. We thank the Transgenic, Knockout and Micro-Injection Core at Washington University in St. Louis, as well as Dr. J. Michael White for helping with generation of the *Cebpa* +37 kb enhancer deletion mouse. This work was supported by the grants from the NIH (R01AI150297, R01CA248919, and R21AI164142, R01AI162643, and R21AI163421 to K.M.M.) and a gift from the 1440 foundation to K.M.M.

1. R. T. Palframan *et al.*, Inflammatory chemokine transport and presentation in HEV: A remote control mechanism for monocyte recruitment to lymph nodes in inflamed tissues. *J. Exp. Med.* **194**, 1361–1373 (2001).
2. F. Geissmann, S. Jung, D. R. Littman, Blood monocytes consist of two principal subsets with distinct migratory properties. *Immunity* **19**, 71–82 (2003).
3. C. Auffray *et al.*, Monitoring of blood vessels and tissues by a population of monocytes with patrolling behavior. *Science* **317**, 666–670 (2007).
4. A. Mildner *et al.*, Genomic characterization of murine monocytes reveals C/EBPβ transcription factor dependence of Ly6C-cells. *Immunity* **46**, 849–862.e7 (2017).
5. J. Hettinger *et al.*, Origin of monocytes and macrophages in a committed progenitor. *Nat. Immunol.* **14**, 821–830 (2013).
6. S. Kawamura *et al.*, Identification of a human clonogenic progenitor with strict monocyte differentiation potential: A counterpart of mouse cMoPs. *Immunity* **46**, 835–848.e4 (2017).
7. A. A. Patel *et al.*, The fate and lifespan of human monocyte subsets in steady state and systemic inflammation. *J. Exp. Med.* **214**, 1913–1923 (2017).
8. S. Yona *et al.*, Fate mapping reveals origins and dynamics of monocytes and tissue macrophages under homeostasis. *Immunity* **38**, 79–91 (2013).
9. M. Guilliams, A. Mildner, S. Yona, Developmental and functional heterogeneity of monocytes. *Immunity* **49**, 595–613 (2018).
10. Z. Liu *et al.*, Fate mapping via Ms4a3-expression history traces monocyte-derived cells. *Cell* **178**, 1509–1525.e19 (2019).
11. S. Menezes *et al.*, The heterogeneity of Ly6Chi monocytes controls their differentiation into iNOS+ macrophages or monocyte-derived dendritic cells. *Immunity* **45**, 1205–1218 (2016).
12. C. G. Briseño *et al.*, Distinct transcriptional programs control cross-priming in classical and monocyte-derived dendritic cells. *Cell Rep.* **15**, 2462–2474 (2016).
13. C. Cheong *et al.*, Microbial stimulation fully differentiates monocytes to DC-SIGN/CD209(+) dendritic cells for immune T cell areas. *Cell* **143**, 416–429 (2010).
14. C. Auffray *et al.*, CX3CR1+ CD115+ CD135+ common macrophage/DC precursors and the role of CX3CR1 in their response to inflammation. *J. Exp. Med.* **206**, 595–606 (2009).
15. C. Varol *et al.*, Monocytes give rise to mucosal, but not splenic, conventional dendritic cells. *J. Exp. Med.* **204**, 171–180 (2007).
16. J. Gamrekelashvili *et al.*, Regulation of monocyte cell fate by blood vessels mediated by Notch signalling. *Nat. Commun.* **7**, 12597 (2016).
17. J. Gamrekelashvili *et al.*, Notch and TLR signaling coordinate monocyte cell fate and inflammation. *Elife* **9**, e57007 (2020).
18. K. W. O'Connor *et al.*, Bcl 6, Irf2, and Notch2 promote nonclassical monocyte development. *Proc. Natl. Acad. Sci. U.S.A.* **120**, e2220853120 (2023).
19. L. Landsman *et al.*, CX3CR1 is required for monocyte homeostasis and atherogenesis by promoting cell survival. *Blood* **113**, 963–972 (2009).
20. L. M. Carlin *et al.*, Nr4a1-dependent Ly6C(low) monocytes monitor endothelial cells and orchestrate their disposal. *Cell* **153**, 362–375 (2013).
21. R. N. Hanna *et al.*, Patrolling monocytes control tumor metastasis to the lung. *Science* **350**, 985–990 (2015).
22. P. B. Narasimhan *et al.*, Patrolling monocytes control NK cell expression of activating and stimulatory receptors to curtail lung metastases. *J. Immunol.* **204**, 192–198 (2020).
23. G. D. Thomas *et al.*, Deleting an Nr4a1 super-enhancer subdomain ablates Ly6C(low) monocytes while preserving macrophage gene function. *Immunity* **45**, 975–987 (2016).
24. D. K. Fogg *et al.*, A clonogenic bone marrow progenitor specific for macrophages and dendritic cells. *Science* **311**, 83–87 (2006).
25. E. W. Scott, M. C. Simon, J. Anastasi, H. Singh, Requirement of transcription factor PU.1 in the development of multiple hematopoietic lineages. *Science* **265**, 1573–1577 (1994).
26. D. Kurotaki *et al.*, Essential role of the IRF8-KLF4 transcription factor cascade in murine monocyte differentiation. *Blood* **121**, 1839–1849 (2013).
27. J. K. Alder *et al.*, Kruppel-like factor 4 is essential for inflammatory monocyte differentiation in vivo. *J. Immunol.* **180**, 5645–5652 (2008).
28. M. W. Feinberg *et al.*, The Kruppel-like factor KLF4 is a critical regulator of monocyte differentiation. *EMBO J.* **26**, 4138–4148 (2007).
29. D. Kurotaki *et al.*, IRF8 inhibits C/EBPα activity to restrain mononuclear phagocyte progenitors from differentiating into neutrophils. *Nat. Commun.* **5**, 4978 (2014).
30. D. A. Anderson, F. Ou, S. Kim, T. L. Murphy, K. M. Murphy, Transition from cMyc to L-Myc during dendritic cell development coordinated by rising levels of IRF8. *J. Exp. Med.* **219**, e20211483 (2022).
31. R. N. Hanna *et al.*, The transcription factor NR4A1 (Nur77) controls bone marrow differentiation and the survival of Ly6C- monocytes. *Nat. Immunol.* **12**, 778–785 (2011).
32. A. Tamura *et al.*, Accelerated apoptosis of peripheral blood monocytes in Cebpb-deficient mice. *Biochem. Biophys. Res. Commun.* **464**, 654–658 (2015).
33. A. Tamura *et al.*, C/EBPbeta is required for survival of Ly6C(-) monocytes. *Blood* **130**, 1809–1818 (2017).
34. A. Wölfler *et al.*, Lineage-instructive function of C/EBPα in multipotent hematopoietic cells and early thymic progenitors. *Blood* **116**, 4116–4125 (2010).
35. D. E. Zhang *et al.*, Absence of granulocyte colony-stimulating factor signaling and neutrophil development in CCAAT enhancer binding protein alpha-deficient mice. *Proc. Natl. Acad. Sci. U.S.A.* **94**, 569–574 (1997).
36. R. Avellino *et al.*, An autonomous CEBPA enhancer specific for myeloid-lineage priming and neutrophilic differentiation. *Blood* **127**, 2991–3003 (2016).
37. H. Guo, S. Cooper, A. D. Friedman, In vivo deletion of the Cebpa +37 kb enhancer markedly reduces Cebpa mrna in myeloid progenitors but not in non-hematopoietic tissues to impair granulopoiesis. *PLoS One* **11**, e0150809 (2016).

38. K. Ikuta, I. L. Weissman, Evidence that hematopoietic stem cells express mouse c-kit but do not depend on steel factor for their generation. *Proc. Natl. Acad. Sci. U.S.A.* **89**, 1502–1506 (1992).
39. K. Akashi, D. Traver, T. Miyamoto, I. L. Weissman, A clonogenic common myeloid progenitor that gives rise to all myeloid lineages. *Nature* **404**, 193–197 (2000).
40. A. Yáñez *et al.*, Granulocyte-monocyte progenitors and monocyte-dendritic cell progenitors independently produce functionally distinct monocytes. *Immunity* **47**, 890–902.e4 (2017).
41. C. F. Calkhoven, C. Müller, A. Leutz, Translational control of C/EBPα and C/EBPβ isoform expression. *Genes Dev.* **14**, 1920–1932 (2000).
42. P. Kirstetter *et al.*, Modeling of C/EBPalpha mutant acute myeloid leukemia reveals a common expression signature of committed myeloid leukemia-initiating cells. *Cancer Cell* **13**, 299–310 (2008).
43. J. S. Jakobsen *et al.*, Mutant CEBPA directly drives the expression of the targetable tumor-promoting factor CD73 in AML. *Sci. Adv.* **5**, eaaw4304 (2019).
44. G. Hoeffel, F. Ginhoux, Ontogeny of tissue-resident macrophages. *Front. Immunol.* **6**, 486 (2015).
45. G. Hoeffel *et al.*, C-Myb(+) erythro-myeloid progenitor-derived fetal monocytes give rise to adult tissue-resident macrophages. *Immunity* **42**, 665–678 (2015).
46. E. Gomez Perdiguero *et al.*, Tissue-resident macrophages originate from yolk-sac-derived erythro-myeloid progenitors. *Nature* **518**, 547–551 (2015).
47. K. E. McGrath *et al.*, Distinct sources of hematopoietic progenitors emerge before HSCs and provide functional blood cells in the mammalian embryo. *Cell Rep.* **11**, 1892–1904 (2015).
48. K.-W. Kim *et al.*, MHC II+ resident peritoneal and pleural macrophages rely on IRF4 for development from circulating monocytes. *J. Exp. Med.* **213**, 1951–1959 (2016).
49. C. Goudot *et al.*, Aryl hydrocarbon receptor controls monocyte differentiation into dendritic cells versus macrophages. *Immunity* **47**, 582–596.e6 (2017).
50. J. Villar *et al.*, ETV3 and ETV6 enable monocyte differentiation into dendritic cells by repressing macrophage fate commitment. *Nat. Immunol.* **24**, 84–95 (2023).
51. V. Heath *et al.*, C/EBPalpha deficiency results in hyperproliferation of hematopoietic progenitor cells and disrupts macrophage development in vitro and in vivo. *Blood* **104**, 1639–1647 (2004).
52. M. Zembala, W. Uracz, I. Ruggiero, B. Mytar, J. Pryjma, Isolation and functional characteristics of FcR+ and FcR- human monocyte subsets. *J. Immunol.* **133**, 1293–1299 (1984).
53. B. Passlick, D. Flieger, H. W. Ziegler-Heitbrock, Identification and characterization of a novel monocyte subpopulation in human peripheral blood. *Blood* **74**, 2527–2534 (1989).
54. H. W. Ziegler-Heitbrock *et al.*, The novel subset of CD14+/CD16+ blood monocytes exhibits features of tissue macrophages. *Eur. J. Immunol.* **23**, 2053–2058 (1993).
55. G. Fingerle *et al.*, The novel subset of CD14+/CD16+ blood monocytes is expanded in sepsis patients. *Blood* **82**, 3170–3176 (1993).
56. W. A. Nockher, L. Bergmann, J. E. Scherberich, Increased soluble CD14 serum levels and altered CD14 expression of peripheral blood monocytes in HIV-infected patients. *Clin. Exp. Immunol.* **98**, 369–374 (1994).
57. A. Rivier *et al.*, Blood monocytes of untreated asthmatics exhibit some features of tissue macrophages. *Clin. Exp. Immunol.* **100**, 314–318 (1995).
58. N. Thieblemont, L. Weiss, H. M. Sadeghi, C. Estcourt, N. Haeffner-Cavaillon, CD14lowCD16high: A cytokine-producing monocyte subset which expands during human immunodeficiency virus infection. *Eur. J. Immunol.* **25**, 3418–3424 (1995).
59. S. Jung *et al.*, Analysis of fractalkine receptor CX(3)CR1 function by targeted deletion and green fluorescent protein reporter gene insertion. *Mol. Cell. Biol.* **20**, 4106–4114 (2000).
60. C. Sunderkötter *et al.*, Subpopulations of mouse blood monocytes differ in maturation stage and inflammatory response. *J. Immunol.* **172**, 4410–4417 (2004).
61. M. A. Ingersoll *et al.*, Comparison of gene expression profiles between human and mouse monocyte subsets. *Blood* **115**, e10-9 (2010).
62. D. Wang, J. D'Costa, C. I. Civin, A. D. Friedman, C/EBPalpha directs monocytic commitment of primary myeloid progenitors. *Blood* **108**, 1223–1229 (2006).
63. C. van Oevelen *et al.*, C/EBPα activates pre-existing and de novo macrophage enhancers during induced pre-B cell transdifferentiation and myelopoiesis. *Stem Cell Rep.* **5**, 232–247 (2015).
64. L. C. Jones *et al.*, Expression of C/EBPbeta from the C/ebpalpha gene locus is sufficient for normal hematopoiesis in vivo. *Blood* **99**, 2032–2036 (2002).
65. J. J. Smink *et al.*, Transcription factor C/EBPbeta isoform ratio regulates osteoclastogenesis through MafB. *EMBO J.* **28**, 1769–1781 (2009).
66. P. Descombes, U. Schibler, A liver-enriched transcriptional activator protein, LAP, and a transcriptional inhibitory protein, LIP, are translated from the same mRNA. *Cell* **67**, 569–579 (1991).
67. K. Wethmar *et al.*, C/EBPbetaDeltauORF mice–a genetic model for uORF-mediated translational control in mammals. *Genes Dev.* **24**, 15–20 (2010).
68. X. Huang *et al.*, Differential usage of transcriptional repressor Zeb2 enhancers distinguishes adult and embryonic hematopoiesis. *Immunity* **54**, 1417–1432.e7 (2021).
69. A. T. Satpathy *et al.*, Zbtb46 expression distinguishes classical dendritic cells and their committed progenitors from other immune lineages. *J. Exp. Med.* **209**, 1135–1152 (2012).
70. S. Kim *et al.*, High amount of transcription factor IRF8 engages AP1-IRF composite elements in enhancers to direct type 1 conventional dendritic cell identity. *Immunity* **53**, 759–774.e9 (2020).
71. S. Kim *et al.*, IL-6 selectively suppresses cDC1 specification via C/EBPβ. *J. Exp. Med.* **220**, e20221757 (2023).
72. T.-T. Liu *et al.*, Ablation of cDC2 development by triple mutations within the Zeb2 enhancer. *Nature* **607**, 142–148 (2022).
73. J.-S. Roe, F. Mercan, K. Rivera, D. J. Pappin, C. R. Vakoc, BET bromodomain inhibition suppresses the function of hematopoietic transcription factors in acute myeloid leukemia. *Mol. Cell* **58**, 1028–1039 (2015).
74. S. Morita, T. Kojima, T. Kitamura, Plat-E: An efficient and stable system for transient packaging of retroviruses. *Gene Ther.* **7**, 1063–1066 (2000).
75. S. Kim, J. Chen, K. M. Murphy, Data from "Transcription factor C/EBPα is required for the developement of Ly6C^{hi} monocytes but not Ly6C^{lo} monocytes". NCBI. https://www.ncbi.nlm.nih.gov/geo/query/acc.cgi?acc=GSE254202. Deposited 25 January 2024.